Accepted Manuscript

Pharmaceutical film coating catalogue for spectral-domain optical coherence tomography

Hungyen Lin, Yue Dong, Daniel Markl, Zijian Zhang, Yaochun Shen, J. Axel Zeitler

PII: S0022-3549(17)30424-0

DOI: 10.1016/j.xphs.2017.05.032

Reference: XPHS 835

To appear in: *Journal of Pharmaceutical Sciences*

Received Date: 22 February 2017

Revised Date: 19 May 2017

Accepted Date: 24 May 2017

Please cite this article as: Lin H, Dong Y, Markl D, Zhang Z, Shen Y, Zeitler JA, Pharmaceutical film coating catalogue for spectral-domain optical coherence tomography, *Journal of Pharmaceutical Sciences* (2017), doi: 10.1016/j.xphs.2017.05.032.

Pharmaceutical film coating catalogue for spectral-domain optical coherence tomography

Hungyen Lin[1], Yue Dong[2], Daniel Markl[3], Zijian Zhang[2], Yaochun Shen[2], and J. Axel Zeitler[3]

[1] Department of Engineering, Lancaster University, Lancaster LA1 4YW, UK
[2]Department of Electrical Engineering and Electronics, University of Liverpool, Liverpool L69 3GJ, UK
[3]Department of Chemical Engineering and Biotechnology, University of Cambridge, Cambridge CB2 0AS, UK

*Corresponding author: h.lin2@lancaster.ac.uk, y.c.shen@liverpool.ac.uk and jaz22@cam.ac.uk

Abstract

Optical coherence tomography (OCT) has recently been demonstrated to measure the film coating thickness of pharmaceutical tablets and pellets directly. The results enable the analysis of inter- and intra-tablet coating variability at an off-line and in-line setting. To date, only a few coating formulations have been tried and there is very little information on the applicability of OCT to other coatings. As it is well documented that optical methods including OCT are prone to scattering leading to limited penetration, some pharmaceutical coatings may not be measurable altogether. This study presents OCT measurements of 22 different common coatings for the assessment of OCT applicability.

Keywords: optical coherence tomography; pharmaceutical film coating; coating thickness.

1. Introduction

Film coatings serve the very purpose of achieving colour uniformity, light protection, and taste masking. Coatings are additionally used to modify the drug release or to incorporate an active pharmaceutical ingredient in the formulation. Coating quality can be studied either by numerical modelling [1] or by the aid of process analysers. Various process analytical technology (PAT) approaches have been demonstrated for characterising pharmaceutical coating, which include NIR and Raman spectroscopy [2-4], nuclear magnetic resonance imaging [5], terahertz pulsed imaging (TPI) [6-8] and optical coherence tomography (OCT) [9-15]. Amongst these methods, TPI and OCT are attractive because they offer a direct, calibration-free coating thickness measurement, where the only unknown is the coating refractive index that can be obtained as a one-off measurement with terahertz time-domain spectroscopy and spectroscopic ellipsometry, respectively. Comparing the two, TPI has limited resolution (i.e., a lateral spatial of 200 μm and axial (depth) resolution of 2 μm for coating thickness greater than 30-40 μm) and requires relatively long measurement times (in the range of 8 ms). OCT in contrast, can achieve sub-μm resolutions for coating thickness greater than 10 μm and exploits an μs acquisition time leading to information on both inter-tablet and intra-tablet coating variation. Specifically, OCT has been demonstrated in an off-line [9-11] and in-line setting for characterising pellets [12, 13] and

tablets [14, 15]. However, OCT has limited penetration depth than TPI, and in some cases fails to image through coatings altogether. This limitation originates from a similar refractive index between the tablet core and coating leading to weaker reflections, and/or pronounced scattering encountered as the optical beam penetrates into the sample, resulting in substantial signal attenuation. These effects ultimately limit the resolvable coating thickness. There is currently very little information available in the literature on what coating materials can or cannot be imaged through using OCT technology. This study therefore aims to examine the transparency of a range of coating formulations for OCT measurement at 840 nm.

2. Materials and Methods

2.1 Tablet Production

The samples used in the present work comprise 22 randomly selected tablets from 22 different batches where a different coating formulation was used for each of the batches. The coating product name, the corresponding alias and photographs of the tablets are shown in Table 1. Coating materials were applied to bi-convex shaped tablet cores that contained 50% lactose monohydrate and 50% microcrystalline cellulose. Film coating was performed with a 15" fully perforated Labcoat IIX (O'Hara Technologies Inc., Canada) equipped with one spray nozzle (970 Düsen-Schlick GmbH, Untersiemau, Germany). The coating pan has a diameter of 380 mm and a full volume of 4.5 L enabling a batch size of 500 g. Average thickness, diameter and weight of the tablet cores (n=6) was 4.079 ± 0.018 mm, 10.069 ± 0.005 mm and 321 ± 3 mg, respectively. For measurement comparisons, one side of the tablets was marked by a scratch mark to serve as a datum. Film coating thickness was estimated by measuring the physical dimensions of coated tablets with a micrometre gauge and subtracting it away from the average core thickness, assuming no dimensional changes to the cores in the coating process.

2.2 Spectral-domain optical coherence tomographic measurements

An in-house fiber based spectral-domain OCT system [16] was developed for B-scan measurements of the coated tablets. As shown in Fig. 1, a super-luminescent diode (EXALOS AG, Schlieren, Switzerland), centred at a wavelength of 840 nm with a full width at half maximum (FWHM) bandwidth of 55 nm was used as the light source. The light source provided a theoretical axial resolution of 5.7 μm in air. The collimated light beam was firstly coupled into the input port of a 2 x 2 wideband single mode fiber coupler using a collimator. The light beam was subsequently split (50:50) into a reference and a probe beam. The reference beam was collimated by an adjustable collimator (CFC-2X-B, Thorlabs Inc., USA) and reflected by a reference mirror. The probe beam was focused onto the tablet surface by another identical adjustable collimator. The focal length was 7 mm, which lead to a lateral resolution of 20 μm and a depth of field of 734 μm. The back-scattered probe beam interfered with the reflected reference beam at the output port of the fiber coupler. The interferogram was collected by a high resolution spectrometer (Wasatch Photonics Inc., Logan, Utah) consisting of 2048 pixels linear array CCD camera. In order to obtain a B-scan (cross-sectional image) across the tablet

surface, a translation stage was used to move the tablet sample at a velocity of 1 mm/s by a motorised stage. The spectrometer was set to acquire a spectrum every 6 ms with an exposure time of 90 µs. In total, one thousand A-scans, which covered a length of 6 mm with an equivalent step size of 6 µm, were acquired for each tablet to generate a B-scan. The measured optical spot size on the tablet surface was approximately 20 µm. Measurements were performed perpendicular to the overall tablet surface plane at the tablet centre as opposed to being perpendicular to the tablets' curved surface [6, 7]. As such, only the coating thickness at the tablet central region can be accurately measured unless the tablet curvature is accounted for [17]. The coating thickness is proportional to the separation between adjacent reflection peaks in an A-scan and is determined using $d = \Delta tc/(2n)$, where d is the coating thickness, c is the speed of light, Δt is the peak separation, and n is the coating refractive index.

2.3 X-ray computed microtomography

X-ray computed microtomography (XµCT) measurement was performed on a Skyscan 1172 (Bruker, Kontich, Belgium, control software: Skyscan1172 XµCT Control Program v1.5). Reconstruction was performed using the program NRecon (Bruker, v1.6.9.8) on a single PC using GPU accelerated reconstruction (Windows 7 64-bit workstation, 2 Intel Xeon X5647 with 4 cores each, 48 GB RAM, NVIDIA Quadro 4000 with 256 cores) yielding 3D data with an isotropic voxel size of 0.95 µm. The data acquisition time was 4 hours and the image reconstruction took 0.5 h size for 433 slices of 1116 x 1116 pixels.

3. Results and Discussions

Figure 2 shows the acquired B-scans of the 22 coated tablets. Evidently, the coating–core interface for coatings 1, 2, 7, 8, 13 and 18 can be visibly observed. The level of contrast between the air-coating and coating-core interface in coatings 1, 4 and 13 may be enhanced with signal denoising [16]. It should be noted that in order to quantify the absolute coating thickness, a clear observation of the coating-core interface and knowledge of the coating refractive index is required [16, 17]. As refractive index remains unknown in this study, coating thickness is not determined but instead, estimated using a micrometre gauge. As a quick check, we measured coating 9 using XµCT, sub-volume shown in Figure S1, that yielded a thickness of 51.0 ± 6.2 µm (n = 10) in agreement with the estimated thickness of 59 ± 10 µm. No thickness information could be derived with OCT in this instance due to an absence of the coating-core interface. Closer inspection of Figure S1 also shows that some of the coating has fused into the tablet core [18,19], which would have caused a gradual refractive index change leading to low contrast in OCT measurement. To better isolate the causes behind OCT opaqueness at 840 nm, the coating compositions for the respective coatings are listed in Table 2. In coating compositions without pigments or colorants, generally the coating-core interface in B-scans is visible. Coatings 1 and 3, however, are notable exceptions because of the additional lactose and polydextrose, which may have increased scattering and/or reduced the refractive index contrast between the core and coating as the core also contained 50% lactose monohydrate.

This would then reduce the reflected signal intensity from the coating-core interface, resulting in no clear observation of the coating-core interface on the B-scan. Assuming negligible optical absorption in the polymer binder [20], for compositions containing pigments, in particular, titanium dioxide, the coating-core interface is not visible at all. This is due to the pigment particle size and a relatively high value of the effective refractive index that in turn, increases reflection at the air-coating interface meaning that only a fraction of incidence beam can actually penetrate into the coating [20]. As the remaining beam travels through into the coating, more scattering is encountered leading to a further signal reduction for measurement. The scattering effect for yellow iron oxide compared to titanium dioxide is generally weaker at near-infrared wavelengths [21]. Despite this, coating 9 is still opaque to OCT because of the gradual refractive index change encountered because the coating dispersion has penetrated into the core material [18,19]. On the contrary, 3% weight gain red coating (coating 18), is transparent to OCT largely due to a comparatively larger difference between the coating and core refractive index in spite of the increased air-coating reflection from the similar coloured coating to the incident beam [22]. For another red coating (coating 20), the coating-core interface is not visible due to the titanium dioxide used in a comparatively thicker coating (10% weight gain). Finally, it is interesting to note that where the coating contains only talc and dye in the colourant as in the case of coating 13, the coating-core interface is marginally visible in the OCT measurements.

4. Conclusion

With the emergence of OCT for the non-destructive evaluation of pharmaceutical coatings, it is important to know the limitations of the technique. We have presented OCT measurements for a range of pigments and formulations based on a popular immediate release coating platform used in the pharmaceutical industry today. Our findings show that coating transparency for OCT measurement ultimately depends on the pigment type, coating formulation and the tablet core as well as the coating process itself. Our findings further show that where the coating material contains titanium dioxide, either alone or together with other pigments, OCT measurement becomes adversely affected by scattering resulting in a blurred coating-core interface that makes coating thickness quantification impossible. For coatings without titanium dioxide, coating transparency is not always guaranteed. In order to precisely explain our measurements, mechanistic modelling could be applied. We therefore envision that OCT might be best suited for PAT applications of functional polymeric coatings, and in particular for multiparticulates where high pigmentations can be avoided [10-15, 23]. For coatings on tablets where pigments cannot be avoided, TPI is a proven alternative for coating thickness greater than 30-40 μm [6,24].

Acknowledgements
The authors would like to acknowledge the financial support from UK EPSRC Research Grant EP/L019787/1 and EP/L019922/1. The authors acknowledge Colorcon Ltd. (Dartford, UK) for providing the materials used in this study. HL also acknowledges travel support from Joy Welch Educational Charitable Trust.

References

1. Suzzi D, Toschkoff G, Radl S, Machold D, Fraser SD, Glasser BJ, Khinast JG. 2012. DEM simulation of continuous tablet coating: Effects of tablet shape and fill level on inter-tablet coating variability. Chem Eng Sci 69:107–121.

2. Romero-Torres S, Pérez-Ramos JD, Morris KR, Grant ER 2005. Raman spectroscopic measurement of tablet-to-tablet coating variability. J Pharm Biomed Anal 38(2):270-274.

3. McGoverin CM, Rades T, Gordon KC 2008. Recent pharmaceutical applications of Raman and terahertz spectroscopies. J Pharm Sci 97:4598-4621.

4. Ricci C, Nyadong L, Fernandez FM, Newton PN, Kazarian SG 2007. Combined Fourier-transform infrared imaging and desorption electrospray-ionization linear ion-trap mass spectrometry for analysis of counterfeit antimalarial tablets. Anal Bioanal Chem 387:551-559.

5. Djemai A, Sinka IC 2006. NMR imaging of density distributions in tablets. Int J Pharm 319:55-62.

6. Zeitler JA, Shen Y, Baker C, Taday PF, Pepper M, Rades T 2007. Analysis of coating structures and interfaces in solid oral dosage forms by three dimensional terahertz pulsed imaging. J Pharm Sci 96:330-340.

7. Zeitler JA, Gladden LF 2009. In-vitro tomography and non-destructive imaging at depth of pharmaceutical solid dosage forms. Eur J Pharm Biopharm 71:2-22.

8. Lin H, May RK, Evans MJ, Zhong S, Gladden LF, Shen YC, Zeitler JA 2015. Impact of Processing Conditions on Inter-tablet Coating Thickness Variations Measured by Terahertz In-Line Sensing. J Pharm Sci 104(8): 2513–2522.

9. Mauritz JM, Morrisby RS, Hutton RS, Legge CH, Kaminski CF 2010. Imaging pharmaceutical tablets with optical coherence tomography. J Pharm Sci 99:385-391.

10. Zhong S, Shen Y-C, Ho L, May RK, Zeitler JA, Evans M, Taday PF, Pepper M, Rades T, Gordon KC, Müller R, Kleinebudde P 2011. Non-destructive quantification of pharmaceutical tablet coatings using terahertz pulsed imaging and optical coherence tomography. Optics and Lasers in Engineering 49:361-365.

11. Koller DM, Hannesschlager G, Leitner M, Khinast JG 2011. Non-destructive analysis of tablet coatings with optical coherence tomography. Eur J Pharm Sci 44:142-148.

12. Li C, Zeitler JA, Dong Y, Shen YC 2014. Non-destructive evaluation of polymer coating structures on pharmaceutical pellets using full-field optical coherence tomography. J Pharm Sci 103:161-166.

13. Markl D, Zettl M, Hannesschläger G, Sacher S, Leitner M, Buchsbaum A, Khinast JG 2015. Calibration-free in-line monitoring of pellet coating processes via optical coherence tomography. Chemical Engineering Science 125:200-208.

14. Markl D, Hannesschläger G, Sacher S, Leitner M, Khinast JG 2014. Optical coherence tomography as a novel tool for in-line monitoring of a pharmaceutical film-coating process. Eur J Pharm Sci 55(0):58-67.

15. Markl D, Hannesschläger G., Sacher S, Leitner M, Buchsbaum A, Pescod R, Baele T, Khinast JG 2015, In-Line Monitoring of a Pharmaceutical Pan Coating Process by Optical Coherence Tomography. J Pharm Sci 104(8): 2531–2540.

16. Lin H, Dong Y, Shen YC Zeitler JA 2015. Quantifying Pharmaceutical Film Coating with Optical Coherence Tomography and Terahertz Pulsed Imaging: An Evaluation. J Pharm Sci 104(10): 3377–3385.

17. Markl D HG, Sacher S, Leitner M, Khinast JG, Buchsbaum A 2015. Automated pharmaceutical tablet coating layer evaluation of optical coherence tomography images. Measurement Science and Technology 26:035701.

18. Ruotsalainen M, Heinämäki J, Guo H, Laitinen N, Yliruusi J 2003. A novel technique for imaging film coating defects in the film-core interface and surface of coated tablets. Eur. J. Pharm. Sci. 56(3):381-388.

19. Pourkavoos N, Peck GE 1993. The Effect of Swelling Characteristics of Superdisintegrants on the Aqueous Coating Solution Penetration into the Tablet Matrix During the Film Coating Process. Pharm Res. 10(9):1363-1371.

20. Song J, Qin J, Qu J, Song Z, Zhang W, Xue X, Shi Y, Zhang T, Ji W, Zhang R, Zhang H, Zhang Z, Wu X 2014. The effects of particle size distribution on the optical properties of titanium dioxide rutile pigments and their applications in cool non-white coatings, Sol. Mater. Sol. Cells, 130: 42-50.

21. Levinson R, Berdahl P, Akbari H 2005. Solar spectral optical properties of pigments – Part II: survey of common colorants, Sol. Energy Mater. Sol. Cells 89(4): 351–389.

22. Levinson R, Berdahl P, Akbari H 2005. Solar spectral optical properties of pigments—Part I: Model for deriving scattering and absorption coefficients from transmittance and reflectance measurements, Sol. Mater. Sol. Cells 89(4): 319–349.

23. Lin H, Dong Y, Markl D, Williams BM, Zheng Y, Shen YC, Zeitler JA 2017. Measurement of the inter-tablet coating uniformity of a pharmaceutical pan coating process with combined terahertz and optical coherence tomography in-line sensing. J Pharm Sci 106(4): 1075-1084.

24. May RK, Evans MJ, Zhong S, Warr I, Gladden LF, Shen Y, Zeitler JA 2011. Terahertz in-line sensor for direct coating thickness measurement of individual tablets during film coating in real-time. J Pharm Sci 100(4):1535-1544.

Figure 1 - Schematic of an in-house SD-OCT system with a tablet placed in the perforated coating pan. SLD - superluminescent diode, RM – reference mirror, C1 and C2 – adjustable collimators

Figure 2 – B-scans of the coated tablets coated where the air-coating interface can be observed and the coating-core interface is only visible for only coatings 1, 2, 7, 8, 13 and 18.

Table 1 – Images of the tablets coated with the respective coating product and the corresponding alias.

Table 2 – Coating compositions of the coating aliases with the highlighted rows corresponding to OCT transparency. The weight and tablet thickness were measured of 6 tablets per batch. The coating thickness and weight gain were calculated from the average weight and tablet thickness measurements of each batch and the tablet core. The standard deviation was calculated by applying the error propagation law. HPMC - hydroxypropyl methylcellulose, PEG - polyethylene glycol, PVA - poly(vinyl alcohol), CMC - carboxymethyl cellulose, SLS - sodium lauryl sulfate, HPC - hydroxypropyl cellulose.

Figure S1 – Renderings of a sub-volume from XµCT data of a tablet with coating 9 applied. The coating material (yellow) and the tablet core (red) are shown in a), whereas b) depicts only the coating material.

	Product ID			Product ID			Product ID	
Coating 1	03F190003 (opadry)		Coating 9	03F220071		Coating 17	114F210058	
Coating 2	20A29015 (opadry)		Coating 10	33G200004		Coating 18	114F250049	
Coating 3	31F29070 (opadry II)		Coating 11	03B205020 (opadry)		Coating 19	200F220052	
Coating 4	45F29058 (opadry II)		Coating 12	03F205017		Coating 20	493Z240008	
Coating 5	02A240002 (opadry)		Coating 13	85F205105		Coating 21	TC-117-205006	
Coating 6	02B220014		Coating 14	85G200008		Coating 22	TC-116-205001	
Coating 7	85F190000 (opadry II)		Coating 15	88A210007 (opadry amb II)				
Coating 8	70W29079 (opadry ns-g)		Coating 16	112A210011				

	Nominal weight gain	Measured weight gain (%)	Estimated coating thickness (μm)	Polymer	Plasticizer	Colourants		Auxiliary
						Pigment	Dye	
Coating 1	3%	5.1 ± 1.1	40 ± 3	HPMC	PEG			
Coating 2	3%	5.5 ± 1.1	54 ± 5	HPMC HPC				
Coating 3	3%	6.2 ± 1.1	46 ± 4	HPMC	PEG			Lactose
Coating 4	3%	6.0 ± 1.1	50 ± 3	HPMC	Propylene glycol			Polydextrose
Coating 5	3%	3.4 ± 1.1	47 ± 9	HPMC		Red iron oxide Yellow iron oxide Titanium dioxide Talc		
Coating 6	3%	2.1 ± 1.2	27 ± 13	HPMC	PEG	Yellow iron oxide Titanium dioxide		
Coating 7	3%	5.1 ± 1.2	37 ± 4	PVA	PEG	Talc		
Coating 8	3%	5.7 ± 1.1	41 ± 3	Sodium CMC		Tapioca dextrin		Lecithin Sodium citrate Dextrose
Coating 9	3%	3.6 ± 1.1	59 ± 10	HPMC	PEG	Yellow iron oxide		
Coating 10	3%	3.2 ± 1.4	50 ± 18	HPMC	PEG Triacetin	Yellow iron oxide Black oxide Titanium dioxide		Lactose

Coating 11	3%	3.4 ± 1.0	53 ± 9	HPMC	PEG	Titanium dioxide	Blue	Capmul
Coating 12	3%	3.5 ± 1.1	55 ± 11	HPMC	PEG	Titanium dioxide Talc	Blue	
Coating 13	3%	3.1 ± 1.1	52 ± 10	PVA	PEG	Talc	Blue	
Coating 14	3%	3.4 ± 1.3	47 ± 12	PVA	PEG	Black oxide Carmine Titanium dioxide Talc	Blue	Lecithin
Coating 15	4%	4.3 ± 1.1	52 ± 12	PVA		Titanium dioxide Talc	Cu Chlorophillin	SLS
Coating 16	4%	5.0 ± 1.1	59 ± 10	HPMC HPC		Titanium dioxide Talc	Cu Chlorophillin	
Coating 17	3%	3.3 ± 1.2	60 ± 14	PVA	PEG	Riboflavine Spirilina Veg carbon black Titanium dioxide Talc		
Coating 18	3%	2.2 ± 1.1	28 ± 12	PVA	PEG	Yellow iron oxide Carmine Talc		Polysorbate
Coating 19	4%	6.4 ± 1.4	70 ± 15	PVA Eudragit	PEG	Yellow iron oxide Titanium dioxide Talc	Blue Yellow	
Coating 20	10%	9.9 ± 1.6	105 ± 13	Eudragit		Carmine Titanium dioxide Talc		Poloxamer SLS Sodium bicarbonate Calcium silicate
Coating 21	3%	3.4 ± 1.1	48 ± 10	PVA	PEG	Titanium dioxide Talc	Blue Yellow	Lecithin

Coating 22	3%	3.8 ± 1.2	54 ± 12	HPMC	Propylene glycol	Titanium dioxide	Blue

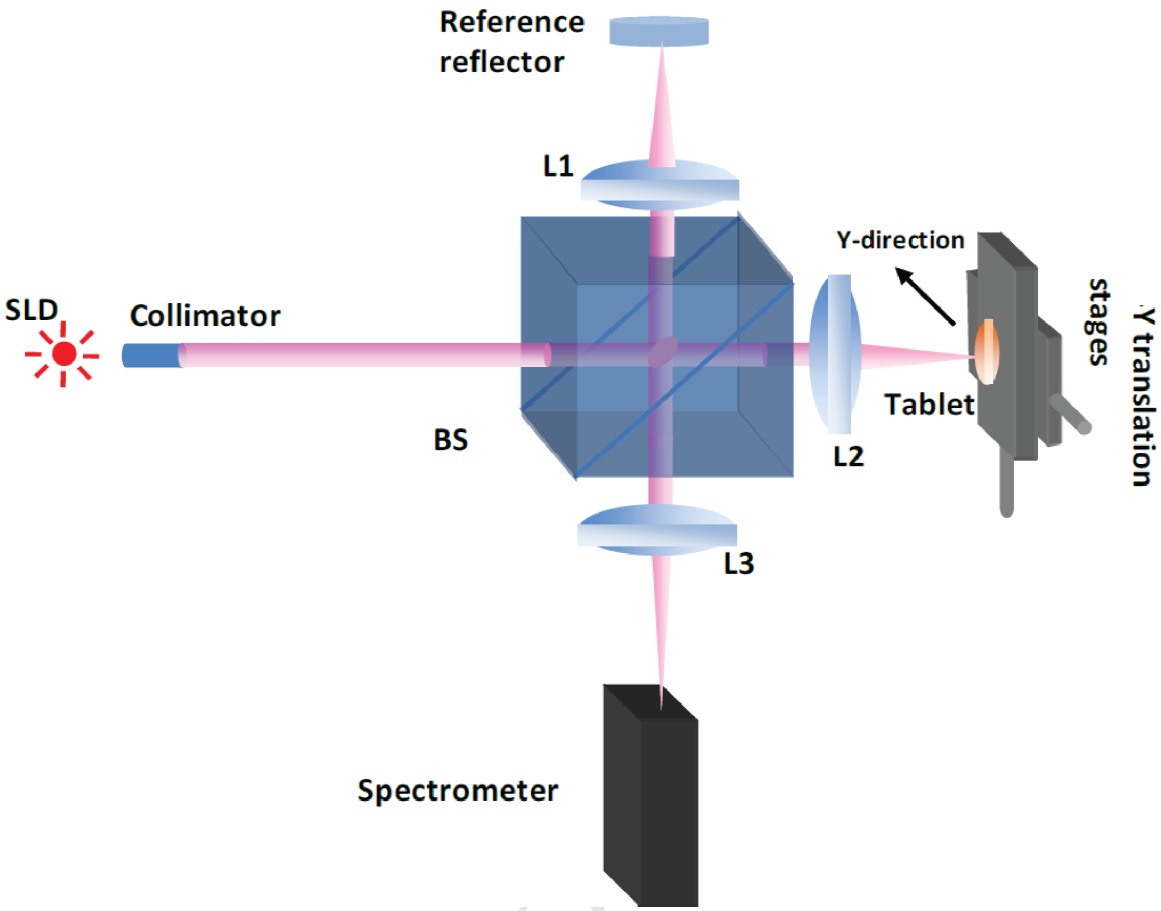
Reference
reflector
L1
Y-direction
SLD
Collimator
Y translation
stages
Tablet
BS
L2
L3
Spectrometer

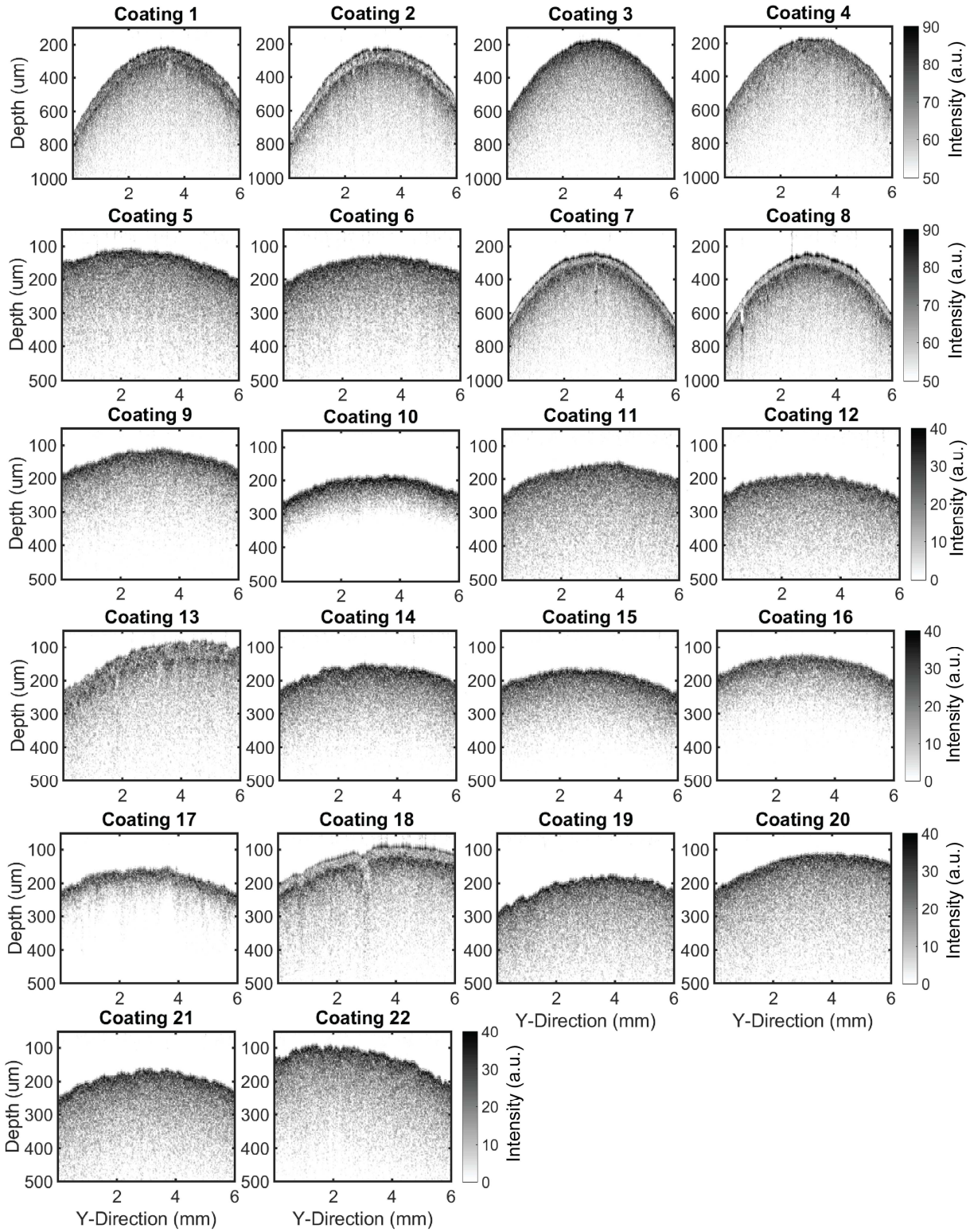
Coating 1
Coating 2
Coating 3
Coating 4
Coating 5
Coating 6
Coating 7
Coating 8
Coating 9
Coating 10
Coating 11
Coating 12
Coating 13
Coating 14
Coating 15
Coating 16
Coating 17
Coating 18
Coating 19
Coating 20
Coating 21
Coating 22
Depth (um)
Y-Direction (mm)
Intensity (a.u.)